RSC Advances

Porous zirconium alginate beads adsorbent for fluoride adsorption from aqueous solutions

Journal:	*RSC Advances*
Manuscript ID:	RA-ART-10-2014-012036.R1
Article Type:	Paper
Date Submitted by the Author:	23-Nov-2014
Complete List of Authors:	zhou, qiusheng; Southwest University of Science and Technology, xiaoyan, lin; Southwest University of Science and Technology, wang, jing; Southwest University of Science and Technology, Luo, Xuegang; Southwest University of Science and Technology, Engineering Research Center of Biomass Materials, Ministry of Education qian, jin; Southwest University of Science and Technology,

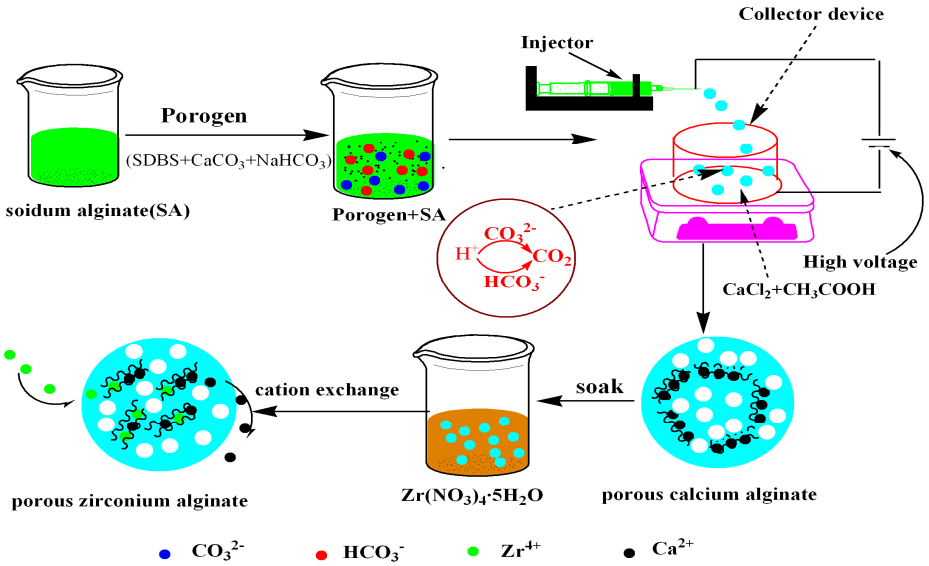

Fig. 1 Schematic diagram of preparation porous zirconium alginate.

The porous zirconium alginate as a novel adsorbent was prepared utilizing high voltage electrostatic spinning device combining the use of inorganic porogen agent from sodium alginate by further loading with zirconium ions. A batch of adsorption experiments were carried out under various conditions: solution pH, adsorbent dose, initial fluoride ion concentration, adsorption temperature and contact time. The result suggested that porous zirconium alginate beads showed well potential for defluorination.

Porous zirconium alginate beads adsorbent for fluoride adsorption from aqueous solutions

ZHOU Qiusheng[1,2], LIN Xiaoyan[1,2*], QIAN Jin[1], WANG Jing[1], LUO Xuegang[2]

(1 *School of Materials Science and Engineering*, *Southwest University of Science and Technology*, *Mianyang* 621010, *Sichuan*, *China*;

2 *Engineering Research Cen ter of Biomass Materials*, *Ministry of Education*, *Mianyang* 621010, *Sichuan*, *China*)

Abstract

Porous zirconium alginate beads as a novel adsorbent were prepared for fluoride removal and characterized by SEM, FTIR, TG, EDX and XPS. The effect of solution pH, adsorbent dose, initial fluoride concentration, contact time, medium temperature and the coexisting ions on adsorption capacity of fluoride ion has been studied. The presence of HCO_3^- , SO_4^{2-} and PO_4^{3-} had a large negative impact on fluoride removal. The kinetics of fluoride ion adsorption onto porous zirconium alginate was followed the pseudo-second-order with correlation of 0.9953. The isotherm data were well fitted to the Langmuir isotherm model and the maximum capacity was 32.797 mg/g. The values of ΔH^0, ΔS^0 and ΔG^0 were calculated and the results indicated that the process of fluoride adsorption was exothermic and spontaneous. The comparison between porous zirconium alginate and other adsorbents suggested that porous zirconium alginate beads possessed a potential for fluoride removal.

Keywords: porous; zirconium; adsorption; fluoride

1 Introduction

Fluoride exists in the environment widely and can enter ground water by natural process. The contamination of ground water with fluoride comes from various industries, such as semiconductor factories, pharmaceutical companies, mines, beryllium extraction plants and aluminum smelters [1]. What's more, intake of excessive fluoride may lead to dental and skeletal fluorosis, neurological damages [2]. Moreover, high concentration of fluoride in ground water has become a worldwide problem. Five million people in Mexico and over 60 million people in China are influenced by fluoride in groundwater [3]. Therefore, removal of fluoride ions from waste water is highly significant for human health.

Fluoride removal from waste water can be achieved by different methods, such as chemical precipitation, ion exchange, adsorption, and reverse osmosis, which have many disadvantages including high installation and maintenance cost [4]. Besides, chemical precipitation induces higher residual fluoride concentration in the effluent. Among these methods, adsorption is one of the most effective and promising method[1]

[1] Corresponding author. Tel.: +86 08166089372; fax: +86 08166089372. *E-mail address: lxy20100205@163.com*.

for fluoride removal of low concentration [5].

Many adsorbents, including activated alumina [6], fly ash [7], zeolite [8], have been tested for defluoridation, while undegradability of inorganic adsorbents after used have a bad effect on the environment after used. In recent years, because of the environmentally friendly of biomass materials, many efforts have been made to investigate and develop naturally available low-cost biomass materials for removing fluoride ion from waste water.

Alginate is a copolymer composed of α-D-annuronate (M) and β-L-guluronate (G) units linked by β-1,4 and α-1,4 glycosidic bonds, with M and G residues present in various proportions and sequences [9]. It is mainly extracted from brown algae or seaweeds [10]. It has attracted much attention on account of its biocompatible and biodegradable property, and rapid gelation ability in many fields. Alginate gelation occurs when divalent cations (Ca^{2+}, Fe^{3+}, Al^{3+}, Zr^{4+}) interact with blocks of G residues, divalent ions diffuse into the sodium alginate solution and replace Na^{+} with a rapid, strong and irreversible formation of gel [11]. Because of high electro negativity and small ionic size, fluoride ion is classified as hard base [12]. Therefore, it has a strong affinity towards electropositive multivalent metal ions like Fe^{3+}, Ca^{2+}, Zr^{4+}, La^{3+}, Ce^{4+}, Al^{3+}. Solidification of positively charged cations onto the material helps to create positive charges which could be used to solidify F^{-} [13]. The characteristic of sodium alginate sol-gel is utilized to load the rare earth element for preparing a novel adsorbent [14], so far, sodium alginate has been successfully immobilize various materials for metal adsorbents, including activated carbon [15], silica nanopowders [16], nanohydroxyapatite [10] , and maghemite nanoparticles [17].

Contacting with the water, some of the powder adsorbents form a stable colloidal suspension, which makes them difficult to separate from the aqueous system. In the actual water treatment, adsorbents are required to pack in a column to remove fluoride from water, powder adsorbents may result in blocking phenomenon, and preparation of bead adsorbents may relieve clogging and post-treatment separation problems [18]. A high voltage electrostatic spinning device is a useful facility to control the average size of beads and satisfy the requirements of large-scale preparation of absorbent. However, the lack of sufficient active sites and the diffusion limitation results in decrease of adsorption rate and adsorption capacity. Therefore, it is necessary to develop novel materials with proper porous structure, more effective for defluoridation [19].

In this study, a novel porous adsorbent for the removal of fluoride from aqueous solution was prepared. In order to investigate the effects of factors on the adsorption performance of adsorbent for fluoride ion, a batch of adsorption experiments were carried out under various conditions: solution pH, adsorbent dose, initial fluoride ion concentration, adsorption temperature and contact time. Moreover, SEM, FTIR, EDX and XPS were utilized to characterize adsorbent, and various adsorption isotherms

and kinetic models were investigated to understand the adsorption process.

2 Experimental

2.1 Materials

Sodium fluoride, sodium sulfate, Sodium metasilicate nonahydrate, sodium alginate, Sodium phorhoate tribaric dodecahydrate, sodium dodecyl benzene sulfonate (SDBS) and zirconium nitrate pentahydrate, calcium carbonate, calcium chloride anhydrous and sodium bicarbonate used in the study were of analytical grade, all of which were purchased from Ke long Co.Ltd without further purification. Stock solution of fluoride was prepared by dissolving 0.7405 g of sodium fluoride in 1L deionized water, and further diluted the required concentrations before used.

2.2 Preparation of porous zirconium alginate adsorbent

0.2% (w/w) of SDBS, 2.5% (w/w) of calcium carbonate, 0.8% (w/w) of sodium bicarbonate and sodium alginate solution of 1.5% (w/w) were mixed, stirred to incorporate air until a stable foam was obtained. The mixed solution was injected by electrostatic spinning machine (DT-200, Dalian ding tong technology development Co.Ltd) into a 3% (w/w) of $CaCl_2$ solution containing 6% (v/v) of acetic acid. The electronic injection conditions were as following: 2% (w/w) of sodium alginate solution 5-10 mL, 2-10 kv of operation electric voltage and 5-15 cm of the collecting distance. After stirred for some time, porous calcium alginate beads were formed, then filtered, washed in deionized water, and subsequently soaked in 3% (w/w) of $Zr(NO_3)_4 \cdot 5H_2O$ solution. Here, the Ca^{2+} of calcium alginate was replaced by metal ions (Zr^{4+}) through cation exchange to produce zirconium alginate. Finally, porous zirconium alginate beads were dried at 40 □ in an air oven. The schematic diagram of preparation of porous zirconium alginate is displayed in Fig. 1.

2.3 Batch adsorption experiments

Adsorption experiments were completed by the batch equilibration method in triplicates. About 0.05 g of dry adsorbent was added into 50 mL of 20 mg/L sodium fluoride solution with a desired pH value. The solution pH was adjusted with 1M HCl and 1M NaOH. The mixture was shaken in a shaker at room temperature. Samples were taken at predetermined time intervals for the analysis of fluoride concentrations in the solution until reaching the adsorption equilibrium. The adsorption capacity of adsorbent was investigated at different conditions including doses of adsorbent, contact time, medium pH, initial fluoride concentrations and temperature. The fluoride adsorption on the adsorbent was studied at different concentrations 20 mg/L, 40 mg/L, 60 mg/L, 80 mg/L, and 100 mg/L of 50 mL solution and in the temperature range of 303.15 K, 308.15 K, 313.15 K, 318.15 K and 323.15 K at optimal pH. The concentration of fluoride was detected by fluoride ion selective electrode pF-1 (Leici, China) before and after adsorption. A equilibrium adsorption capacity of adsorbent was calculated according to the following equations.

$$q_e = \frac{(C_0 - C_e)V}{m} \quad (1)$$

Where q_e is the adsorption capacity of adsorbent (mg/g), C_0 and C_e are initial and equilibrium concentration (mg/L), m (g) is the dry weight of absorbent and V (L) is the volume of fluoride solution.

2.4 Characterization of adsorbent

The surface morphology of the porous zirconium alginate beads was observed by TM 3000 scanning electron microscope. The nitrogen adsorption isotherms were performed in an automated volumetric system (JW-BK300, Beijing subtle Triglobal Science and Technology Corporation). FTIR of the adsorbent was obtained by using FTIR spectrophotometer (Nicolet-5700, PerkinElmer Instruments Corporation) and adopting the KBr tablet method. The element composition and distribution were analyzed by Energy Dispersive X-ray (EDX, Ultra 55, Zesis Corporation) before and after adsorption. The thermogravimetric analysis (TGA) was carried out by thermogravimetric analyzer (United States TA Corporation) in nitrogen atmosphere under the heating rate of 10 □/min varying from room temperature to 800 □. The binding energies of the elements before and after adsorption were obtained by using X-Ray Photoelectron Spectroscopy (XPS, Thermo Scientific Escalab 250, Thermo Fisher Corporation).

3 Results and discussion

3.1 Characteristics of the porous zirconium alginate

3.1.1 Surface morphology analysis

The morphology of porous zirconium alginate before and after adsorption are respectively shown in Fig. 2, which owns the average particle size, 1.969 mm (Fig. 2a) and 1.536 mm (Fig. 2e) , respectively. Many macropores and three-dimensional net structure appeared in the inner of adsorbent with BET surface area of 3.047 m^2/g. Moreover, it was found that the surface of adsorbent changed a little in the adsorption process, which indicated that zirconium alginate beads had outstanding mechanical properties.

3.1.2 FTIR analysis

The FTIR measurement is widely utilized for the structural analysis of an adsorbent, and it can convey the information of various function groups in the adsorbent. As an important method for chemical analysis, it has also been used to investigate the interaction between adsorbent and adsorbate. FT-IR spectra of sodium alginate, porous zirconium alginate beads before and after adsorption are presented in Fig. 3.

Among the adsorption peaks shown in Fig. 3a, a strong and wide band appeared around 3422.3 cm^{-1} is assigned to -OH stretching vibration, and the band at 2926.0 cm^{-1} is due to C-H antisymmetric stretching vibration. Two small bands at 1615.3 cm^{-1} and 1417.4 cm^{-1} is attributed to COO- antisymmetric stretching vibration and

symmetrical stretching vibration, respectively. 1032.5 cm^{-1} indicated C-O stretching vibration of polysaccharide [20]. In Fig. 3b, FTIR spectra of zirconium alginate beads show broad bands at 3413.5 cm^{-1} and 1621.0 cm^{-1} corresponding to -OH stretching as well as antisymmetric stretching vibration bands in carboxyl groups. Whereas, bands near 2928.6 cm^{-1}, 1384.1 cm^{-1}, 1036.6 cm^{-1} are stretching vibrations of C-H, COO-, C-O. A new band at 1735.9 cm^{-1} could be assigned to free carboxyl groups of zirconium alginate, which suggested the existing of O-Zr^{4+}-O [21]. Comparing Fig.3 c with b, it is clearly seen that all characteristic band positions have a small shift after fluoride adsorption, the bands at 1384.1 cm^{-1}, 1036.6 cm^{-1} moved towards higher wavelength indicating the interaction between adsorbent and fluoride [20].

3.1.3 Thermal properties analysis

The relative stability of the materials could be evaluated by thermogravimetric analysis. The TGA-DTA curves for the zirconium alginate from room temperature to 800 □ are shown in Fig. 4. The weight of adsorbent presents a gradual loss trend in the whole process. The weight loss of 12.36% observed in the range of 81.25-204.51 □ is attributed to the evaporation of water in the matrix. This could also be related to the physically and chemically absorbed water molecule. The weight of adsorbent decreased sharply when the temperature exceeded 204.51 □; the weight loss of 49% between 204.51 □ and 463.15 □ may be connected with the preliminary degradation of alginate. The weight of adsorbent decreased gradually when the temperature exceeded 463.15 □, which could be attributed to the further degradation of the adsorbent. It was apparent that the adsorbent had exhibited outstanding thermostability when the operating temperature is below 204.51 □. The similar result was also observed by other researchers in the study of alginate entrapped Fe(□)-Zr(□) binary mixed oxide bead [22].

3.1.4 Energy dispersive X-ray measurement

The EDX analysis results of the samples before and after Zr^{4+} loading reaction are recorded in Fig. 5a and 5b. The element peaks of C, O, Na were observed respectively at the energy values of 0.25 keV, 0.5 keV and 1.05 keV from the EDX spectra of sodium alginate (Fig. 5a). Comparing Fig. 5a with Fig. 5b revealed that the elements of C, O, Ca, Cl and Zr present on the surface of adsorbent, and several new peaks of Zr^{4+} appearing at energy values of 1.8 keV, 2.1 keV, 2.35 keV in EDX spectra of adsorbent. However, the peak of Na^{+} was not observed. This implied that Na^{+} was replaced by Ca^{2+} and Zr^{4+} completely. Obviously, all the above information demonstrated that the Zr^{4+} was successfully loaded on the sodium alginate molecule. Comparing the EDX spectrum before and after adsorption (Fig. 5b and Fig. 5c), the element of F could be observed obviously in the EDX spectrum after adsorption, which implied that F^{-} was adsorbed onto zirconium alginate.

3.1.5 XPS

In order to understand the mechanism of fluoride removal and the interaction between adsorbent and fluoride, XPS of porous zirconium alginate beads before and after fluoride adsorption was conducted, and the results are shown in Fig. 6. Comparing Fig. 6a with Fig. 6b, it was found that there was a new peak which was attributed to F1s in the Fig. 5b, and the binding energy (684.75 ev) could be obtained from the Fig. 6d. Furthermore, from Fig. 6c, it was found that the peak of Zr3d shifted from 182.99 ev to 183.1 ev, which indicated that the interaction between fluoride ion and zirconium ion and fluoride was effectively adsorbed by zirconium alginate [2].

3.2 Influence of pH on adsorption

In most cases, the pH of the medium is an important factor for fluoride adsorption, because the fluoride ion existence forms and the properties of the adsorbents depend on the solution pH [23]. There exists more than 90% of fluoride exists in the free anionic form (F^-) when the solution exceeds 5 [24], while hydrofluoric acid is the predominant species at pH less than 3 [25]. Adsorption result in the pH range from 1-9 is shown in Fig. 7. The result indicated that the maximum adsorption capacity(14.265 mg/g) could be obtained at solution pH 2 of fluoride solution. In an acidic medium, protonation of functional groups of porous zirconium alginate adsorbent and the formation of trace of weak hydrofluoric acid may influence the amount of fluoride adsorption by porous zirconium alginate adsorbent [26]. A tiny fraction of fluoride becomes unavailable for the adsorption at pH lower than 2, leading to the decline of adsorption of fluoride. Similar result was noted by other authors [1]. As pH of the fluoride solution increases from 2 to 9, adsorption capacity decreases from 14.265 mg/g to 11.453 mg/g. This phenomenon may be explained by the competition between hydroxyl ions and fluoride ions in the solution for adsorption sites of the adsorbent at high pH.

3.3 Influence of adsorbent dose on adsorption

The optimum adsorbent dose can be obtained by using different doses ranging from 0.02g to 0.1g. The effect of adsorbent dose on the fluoride removal at pH 2 (±0.02) is presented in Fig. 8. It has been found that fluoride adsorption capacity decreases from 16.121 mg/g to 12.018 mg/g with the increase of adsorbent dose. It may be attributed to the fact that large amounts of adsorption active sites remain unsaturated. In other words, the increase of adsorbent dosage resulted in lower adsorption capacity during the adsorption process. Due to the defluoridation capacity of adsorbent, 0.04 g (14.723 mg/g) was not much different from 0.06 g (14.334 mg/g), 0.05 g of adsorbent dose was considered as the optimum dose for further research.

3.4 Effect of initial fluoride concentration on adsorption

Effect of initial fluoride concentration on the removal of fluoride onto porous zirconium alginate was studied in the specified range of concentration at different temperature. The results are presented in Fig. 9. It was observed that as the fluoride

concentration increased from 20 mg/L to 100 mg/L, adsorption capacity of adsorbent all increased at the range of temperature from 30□ to 50□. The increase of adsorption capacity may be attributed to increase in amount of fluoride ions available for adsorption with the increase of fluoride concentration and a more intensitive interaction between F^- and adsorbent [27].

3.5 Effect of contact time on adsorption

The effect of contact time on the removal of fluoride was investigated. The contact time varied from 0.5-23 h, and the result is shown in Fig. 10. It was observed that adsorption capacity of porous zirconium alginate was improved by increasing contact time from 0.5 h to 20 h. The phenomenon might be attributed that a number of active sites on the surface of adsorbent were available during the initial stage. After that, the adsorption capacity changed little, which might be due to the reason that fluoride ions gathered in the surface of adsorbent and the remaining active sites were difficult to be occupied [28]. Therefore, it was suggested to conduct adsorption experiments for about 20 h of contact time.

3.6 Effect of co-existing anion

The waste water contains some co-existing ions along with fluoride, which may compete with fluoride for the active sites. In this study, several kinds of typical co-existing anion such as HCO_3^-, NO_3^- , Cl^-, SO_4^{2-}, SiO_3^{2-} and PO_4^{3-} on the adsorption process were investigated by adding required amount of $NaHCO_3$, $NaNO_3$, NaCl Na_2SO_4, $Na_2SiO_3 \cdot 9H_2O$ and $Na_3PO_4 \cdot 12H_2O$ to a 50 mL of 20 mg/L fluoride concentration, the results are given in Fig. 11. The various anions at different concentration have different effect on the fluoride adsorption. NO_3^- , Cl^- and SiO_3^{2-} have negligible effects on fluoride adsorption. However, co-existence of HCO_3^- , SO_4^{2-} and PO_4^{3-} influence significantly fluoride removal. The adsorption capacity of adsorbent in the solution decreased obviously with the addition of HCO_3^- , SO_4^{2-} and PO_4^{3-} . The presence of HCO_3^- SO_4^{2-} and PO_4^{3-} has a large negative impact on fluoride removal, the decreased defluorination may be attributed to the lower affinity of zirconium alginate for fluoride and a competition between the fluoride ions and HCO_3^-, SO_4^{2-} and PO_4^{3-} for the active sites. Similar trend was observed when zirconium-Na-attapulgite as an adsorbent was used for fluoride removal [3].

3.7 Adsorption isotherm studies

The study of adsorption isotherms is an extensive method to examine adsorbent performance. It not only provides the information of the feasibility for removing the fluoride, but also expresses the surface properties and affinity of the adsorbent [10]. Langmuir and Freundlich are the most commonly applied isotherms in solid/liquid systems.

The Langmuir model based on the assumption that all the active sites are equivalent and independent indicates the monolayer adsorption process for fluoride onto the uniformity adsorbent surface[29]. The Langmuir adsorption isotherm

equation can be expressed as follows [30].

$$\frac{C_e}{q_e} = \frac{1}{bq_{max}} + \frac{C_e}{q_{max}} \quad \text{(linear)} \qquad (2)$$

$$q_e = \frac{q_{max} b C_e}{1 + bC_e} \quad \text{(nonlinear)} \qquad (3)$$

Where q_e and C_e are respectively the equilibrium adsorption capacity (mg/g) and the equilibrium concentration of fluoride in solution (mg/L), q_{max} is the maximum fluoride adsorption capacity (mg/g), b is the Langmuir isotherm coefficient which is related to the strength of adsorption.

The Freundlich model is an empirical method which assumes that adsorbent owns heterogeneous adsorbing surfaces [31]. The model may be formulated as:

$$\ln q_e = \ln K_F + \frac{\ln C_e}{n} \quad \text{(linear)} \qquad (4)$$

$$q_e = K_F C_e^{1/n} \quad \text{(nonlinear)} \qquad (5)$$

Where K_F and $1/n$ are the constants that are related to the adsorption capacity and the adsorption intensity. Values of K_F and $1/n$ are calculated from the slope and the linear plot of $\ln q_e$ versus $\ln C_e$. $1/n$ representing the heterogeneity factor gives an indication of the favourability and capacity of the adsorption. The values of n>1 demonstrate beneficial adsorption [32].

The values of Langmuir and Freundlich model constants were calculated from the intercept and slope of the respective plots. Comparing the results presented in Table 1 and Fig. 12, it was observed that the values of correlation coefficient (R^2) of Langmuir linear model were higher than that of Freundlich model, and the correlation coefficients (R^2) of two kinds of linear model were higher than those of nonlinear model. All the information implied that the experimental data can fit the Langmuir linear model better, which suggested that the homogeneous distribution of active sites on the surface of adsorbent and fluoride adsorption took place in a monolayer adsorption manner during the process of adsorption [33]. The maximum adsorption capacity (32.797mg/g) was obtained at 40℃.

3.8 Dubinin-Radushkevich (D-R) model

The mechanism of adsorption is not only obtained by means of Langmuir and Freundlich isotherm model but by Dubinin-Radushkevich model. In order to understand the adsorption mechanism, the equilibrium data were tested with Dubinin-Radushkevich model. The linearized form is given as follows [24]:

$$\ln q_e = \ln q_m - K\varepsilon^2 \qquad (6)$$

$$\varepsilon = RT \ln\left(1 + \frac{1}{C_e}\right) \qquad (7)$$

Where q_e is the equilibrium adsorption amounts (mg/g), q_m is the theoretical capacity(mg/g), ε is Polanyi potential, R is universal gas constant (8.314 J/(mol·K)),

C_e the equilibrium concentration of fluoride in solution (mg/L), K is the constant which is related to adsorption energy and can be used to calculate the mean free energy of adsorption (E) in the following relation:

$$E = (2K)^{-1/2} \qquad (8)$$

According to the value of mean free energy of adsorption, the process of adsorption was classified into chemical, physical, and ion exchange. The adsorption process can be divided into physical adsorption (E<8kJ/mol) and chemical adsorption (8kJ/mol<E<16kJ/mol) [34]. The D-R parameters and value of E are shown in Table 2. The value of E for adsorption of fluoride is 0.647 kJ/mol, less than 8 kJ/mol. The fluoride adsorption onto porous zirconium alginate beads seems to be physical adsorption process.

3.9 Kinetic studies

The adsorption kinetic controls the equilibrium time and influences the adsorption mechanism. In order to investigate the adsorption kinetic, two main adsorption kinetic models including the pseudo-first-order and pseudo-second-order rate model were used to fit the data.

The pseudo-first-order kinetic model is represented by the equation

$$\ln(q_e - q_t) = \ln q_e - k_1 t \qquad (9)$$

The pseudo-second-order kinetic model can be written as

$$\frac{t}{q_t} = \frac{1}{k_2 q_e^{\,2}} + \frac{t}{q_e} \qquad (10)$$

Where q_e (mg/g) and q_t (mg/g) are the amount of fluoride ions adsorbed on the adsorbent at equilibrium and any time t, respectively. k_1 and k_2 are respectively the pseudo-first-order rate constant and the pseudo-second-order rate constant (g/(mg·min)). The larger the k_2 value, the slower the reaction rate.

In order to fit the experimental data, linear fitting methods were carried out. Fitting of pseudo-first-order and pseudo-second-order rate model and the kinetic parameters are presented in Fig. 13 and Table 3, respectively. As indicated by the calculated q_e and R^2 values, the pseudo-second-order rate model fitted the experimental results better than pseudo-first-order model, which implied that the adsorption rate of zirconium alginate depend on the active sites rather than the concentration of adsorbate in the solution, and the rate limiting step was controlled by chemical adsorption related to valent forces through sharing or exchanging electrons between the adsorbent and adsorbate [35].

3.10 Effect of temperature and thermodynamic study of fluoride removal

To assess the effect of the temperature on the adsorption of fluoride at different initial concentration, temperature was varied from 30 □ to 50 □ while the contact time was selected as 20 h and the initial concentration of fluoride was changed from 20mg/L to 100mg/L . The result shown in Fig. 14 revealed that the temperature had a

positive effect on fluoride adsorption with the increase of temperature from 30 □ to 50 □.

The thermodymatic parameters for the adsorption process have been calculated using the following equations [35],

$$\ln K_0 = -\frac{\Delta H^0}{R} \times \frac{1}{T} + \frac{\Delta S^0}{R} \quad (13)$$

$$\Delta G^0 = -RT\ln K_0 \quad (14)$$

Where K_0 equals to $q_{max} \times b$ of the Langmuir isotherm, ΔH^0 is the enthalpy change (kJ/mol), ΔS^0 is the entropy change (J/(mol·K)) and ΔG^0 is the Gibbs free energy change in a given process (kJ/mol). The values of ΔH^0 and ΔS^0 can be obtained from the slope and intercept of a plot of $\ln K_0$ vs. $1/T$ and the results are represented in Table 4 and Fig. 15.

ΔG^0 values were estimated as -5.127 kJ/mol, -4.811 kJ/mol, -5.062 kJ/mol, -5.076 kJ/mol and -5.127 kJ/mol at 303.15 K, 308.15 K, 313.15 K, 318.15 K and 323.15 K, respectively. Values of ΔH^0 and ΔS^0 were estimated to be -3.494 kJ/mol and 4.855 J/(mol·K), respectively. The negative values of ΔG^0 indicated that the adsorption of fluoride onto adsorbents was a spontaneous process while the negative ΔH^0 values implied the process of adsorption was exothermic. The positive value of ΔS^0 suggested increased randomness at the solid/liquid interface during adsorption of fluoride [20].

3.11 Mechanism analysis of fluoride adsorption

The adsorption mechanism has played an important role in understanding the adsorbent characteristics and designing its application. In the process of preparing porous zirconium alginate beads, ion exchange reactions between Na^+ and Zr^{4+} make Zr^{4+} entry into the inner of sodium alginate molecule and then form the structures of egg-box. A large number of hydroxy presented in the adsorbent molecule may be protonated and positively charged at low pH, suggesting that porous zirconium alginate removed fluoride by means of the electrostatic adsorption between the positively charged surface and negatively charged fluoride ions. Moreover, Zr^{4+} was considered as hard acid and would prefer to bind with hard base, for example F^-, which was consistent with the result of FTIR, EDX, XPS [5]. The mechanism of fluoride removal is shown in Fig. 16.

3.12 Fluoride desorption studies

The regeneration of porous zirconium alginate is essential to make a cost effective and friendly process. The result of pH effect on fluoride adsorption by porous zirconium alginate beads showed that the adsorption capacity of porous zirconium alginate beads decreased gradually with the increase of pH and was lower in alkaline solution (Fig.7). In order to improve desorption of the adsorbent, the desorption experiments were carried out in NaOH alkaline solution combined with the addition of $Zr(NO_3)_4 \cdot 5H_2O$ activator at room temperature. Regenerants included

NaOH and $Zr(NO_3)_4{\cdot}5H_2O$ were used to regenerate adsorbent. Exhausted porous zirconium alginate beads were immersed in 0.001M NaOH for 1h and washed repeatedly with deionized water, then transferred to a beaker containing 3wt% $Zr(NO_3)_4{\cdot}5H_2O$ undergoing activation for 3h. The desorption efficiency was about 68.65% after two cycles.

3.13 Comparative study with other adsorbents

The comparison of adsorption capacity of various adsorbents for fluoride is shown in Table. 5. The results showed that the porous zirconium alginate in this study was superior to many other adsorbents in terms of adsorption capacity. The possible reasons are: (1) development of adsorption sites for fluoride ions onto the polymer matrices of alginate sodium by Zr loading, (2) increase of the porous structure in the adsorbents. From the comparison between porous and imporous adsorbents, generally, the structure of porous was in favor of fluoride adsorption, which may be related to the reason that porous structure could produce more active sites. Therefore, zirconium alginate could be considered as a new biocompatible adsorbent to remove fluoride.

4 conclusions

The porous zirconium alginate was prepared from sodium alginate loading with zirconium ions by utilizing high voltage electrostatic spinning device combining the use of inorganic porogen agent. The fluoride adsorption from aqueous solutions by porous zirconium alginate depended on solution pH, adsorbent dosage, initial fluoride concentration, temperature and contact time. Optimum adsorption conditions were at pH 2.0, adsorbent dose 0.05 g and contact time 20 h. The coexisting ion, HCO_3^-, SO_4^{2-} and PO_4^{3-} had a negative effect on the fluoride adsorption. Experimental data were well fitted to the Langmuir isotherm model and the presudo-second-order kinetic model. ΔG^0 and ΔH^0 showed that fluoride removal by porous zirconium alginate was exothermic and spontaneous. According to the FTIR, EDX and XPS analysis, kinetic studies and the value of mean free energy, it can be presumed that the physical adsorption and chemical adsorption corporately controlled adsorption stage. Comparative study of adsorption capacities of the adsorbents showed that porous zirconium alginate beads possessed a promising adsorption capacity, and it could be a potentially material to be used in the fluoride removal.

Acknowledgements

This work was supported by "***" item (13zg610301) and Postgraduate Innovation Fund Project by Southwest University of Science and Technology (14ycx015) and Engineering research Center for Biomass Materials of Ministry of Education, China (12zxbx08). Thanks for the technology support of Engineering Research Center of Biomass Materials, Ministry of Education, Southwest University of Science and Technology.

References

[1] Paudyal H, Pangeni B, Inoue K, et al. Adsorptive removal of fluoride from aqueous solution using orange waste loaded with multi-valent metal ions, J. Hazard. Mater. 192 (2011) 676-682.

[2] Wajima T, Umeta Y, Narita S, et al. Adsorption behavior of fluoride ions using a titanium hydroxide-derived adsorbent, Desalination 249 (2009) 323-330.

[3] Zhang G, He Z, Xu W. A low-cost and high efficient zirconium-modified-Na-attapulgite adsorbent for fluoride removal from aqueous solutions, Chem. Eng. J. 183 (2012) 315-324.

[4] Camacho L M, Torres A, Saha D, et al. Adsorption equilibrium and kinetics of fluoride on sol–gel-derived activated alumina adsorbents, J. Colloid Interface Sci. 349 (2010) 307-313.

[5] Viswanathan N, Sundaram C S, Meenakshi S. Removal of fluoride from aqueous solution using protonated chitosan beads, J. Hazard. Mater. 161 (2009) 423-430.

[6] Chatterjee S, De S. Adsorptive removal of fluoride by activated alumina doped cellulose acetate phthalate (CAP) mixed matrix membrane, Sep. Purif. Technol. 125 (2014) 223-238.

[7] Xu X, Li Q, Cui H, et al. Adsorption of fluoride from aqueous solution on magnesia-loaded fly ash cenospheres, Desalination 272 (2011) 233-239.

[8] Sun Y, Fang Q, Dong J, et al. Removal of fluoride from drinking water by natural stilbite zeolite modified with Fe (III), Desalination 277 (2011) 121-127.

[9] Rocher V, Bee A, Siaugue J M, et al. Dye removal from aqueous solution by magnetic alginate beads crosslinked with epichlorohydrin, J. Hazard. Mater. 178 (2010) 434-439.

[10]Googerdchian F, Moheb A, Emadi R. Lead sorption properties of nanohydroxyapatite–alginate composite adsorbents, Chem. Eng. J. 200 (2012) 471-479.

[11] Cheng Y, Lu L, Zhang W, et al. Reinforced low density alginate-based aerogels: Preparation, hydrophobic modification and characterization, Carbohydr. Polym. 88 (2012) 1093-1099.

[12] Desagani Dayananda, Venkateswara R. Sarva, Sivankutty V. Prasad, Jayaraman Arunachalam, Narendra N. Ghosh. Preparation of CaO loaded mesoporous Al_2O_3: Efficient adsorbent for fluoride removal from water, Chem. Eng. J. 248 (2014) 430-439.

[13] Swain S K, Mishra S, Patnaik T, et al. Fluoride removal performance of a new hybrid sorbent of Zr (IV)–ethylenediamine, Chem. Eng. J. 184 (2012) 72-81.

[14] Huo Y, Ding W, Huang X, et al. Fluoride removal by lanthanum alginate bead: Adsorbent characterization and adsorption mechanism, Chin. J. Chem. Eng. 19 (2011) 365-370.

[15] Hassan A F, Abdel-Mohsen A M, Elhadidy H. Adsorption of arsenic by activated carbon, calcium alginate and their composite beads, Int. J. Biol. Macromol. 68 (2014) 125-130.

[16] Soltani R, Khorramabadi G S, Khataee A R, et al. Silica nanopowders/alginate composite for adsorption of lead (II) ions in aqueous solutions, J. Taiwan Inst. Chem. Eng. 45 (2014) 973-980.

[17] Idris A, Ismail N S M, Hassan N, et al. Synthesis of magnetic alginate beads based on maghemite nanoparticles for Pb (II) removal in aqueous solution, J. Ind. Eng. Chem. 18 (2012) 1582-1589.

[18] Tan W S, Ting A S Y. Alginate-immobilized bentonite clay: Adsorption efficacy and reusability for Cu(II) removal from aqueous solution, Bioresour. Technol. 160 (2014) 115–118.

[19] Han J, Du Z, Zou W, et al. Fabrication of interfacial functionalized porous polymer monolith and its adsorption properties of copper ions, J. Hazard. Mater. 276 (2014) 225-231.

[20] Sujana M G, Mishra A, Acharya B C. Hydrous ferric oxide doped alginate beads for fluoride removal: Adsorption kinetics and equilibrium studies, Appl. Surf. Sci. 270 (2013) 767-776.

[21] Paudyal H, Pangeni B, Nath Ghimire K, et al. Adsorption behavior of orange waste gel for some rare earth ions and its application to the removal of fluoride from water, Chem. Eng. J. 195 (2012) 289-296.

[22] Swain S K, Patnaik T, Patnaik P C, et al. Development of new alginate entrapped Fe(III)–Zr(IV) binary mixed

oxide for removal of fluoride from water bodies, Chem. Eng. J. 215 (2013) 763-771.

[23] Ma J, Shen Y, Shen C, et al. Al-doping chitosan-Fe (III) hydrogel for the removal of fluoride from aqueous solutions, Chem. Eng. J. 248 (2014) 98-106.

[24] Deng Y, Nordstrom D K, Blaine McCleskey R. Fluoride geochemistry of thermal waters in Yellowstone National Park: I. Aqueous fluoride speciation, Geochim. Cosmochim. Acta. 75 (2011) 4476-4489.

[25] Paudyal H, Pangeni B, Inoue K, et al. Preparation of novel alginate based anion exchanger from Ulva japonica and its application for the removal of trace concentrations of fluoride from water, Bioresour. Technol. 148 (2013) 221-227.

[26] Chen J H, Xing H T, Guo H X, et al. Preparation, characterization and adsorption properties of a novel 3-aminopropyltriethoxysilane functionalized sodium alginate porous membrane adsorbent for Cr(III) ions, J.

[27] Jagtap S, Yenkie M K N, Labhsetwar N, et al. Defluoridation of drinking water using chitosan based mesoporous alumina, Microporous Mesoporous Mater. 142 (2011) 454-463.

[28] Chen J H, Liu Q L, Hu S R, et al. Adsorption mechanism of Cu(II) ions from aqueous solution by glutaraldehyde crosslinked humic acid-immobilized sodium alginate porous membrane adsorbent, Chem. Eng. J. 173 (2011) 511-519.

[29] Ramdani A, Taleb S, Benghalem A, et al. Removal of excess fluoride ions from Saharan brackish water by adsorption on natural materials, Desalination 250 (2010) 408-413.

[30] Tomar V, Prasad S, Kumar D. Adsorptive removal of fluoride from aqueous media using *Citrus limonum* (lemon) leaf, Microchem. J. 112 (2014) 97-103.

[31] Asgari G, Roshani B, Ghanizadeh G. The investigation of kinetic and isotherm of fluoride adsorption onto functionalize pumice stone, J. Hazard. Mater. 217 (2012) 123-132.

[32] Zhang T, Li Q, Liu Y, et al. Equilibrium and kinetics studies of fluoride ions adsorption on CeO_2/Al_2O_3 composites pretreated with non-thermal plasma, Chem. Eng. J. 168 (2011) 665-671.

[33] Nie Y, Hu C, Kong C. Enhanced fluoride adsorption using Al (III) modified calcium hydroxyapatite, J. Hazard. Mater. 233 (2012) 194-199.

[34] Srivastav A L, Singh P K, Srivastava V, et al. Application of a new adsorbent for fluoride removal from aqueous solutions, J. Hazard. Mater.263 (2013) 342-352.

[35] Deze E G, Papageorgiou S K, Favvas E P, et al. Porous alginate aerogel beads for effective and rapid heavy metal sorption from aqueous solutions: Effect of porosity in Cu2+ and Cd2+ ion sorption, Chem. Eng. J. 209 (2012) 537-546.

[36] Biswas K, Gupta K, Ghosh U C. Adsorption of fluoride by hydrous iron (III)–tin (IV) bimetal mixed oxide from the aqueous solutions, Chem. Eng. J. 149 (2009) 196-206.

[37] Samatya S, Mizuki H, Ito Y, et al. The effect of polystyrene as a porogen on the fluoride ion adsorption of Zr (IV) surface-immobilized resin, React. Funct. Polym. 70 (2010) 63-68.

[38] Wu H X, Wang T J, Chen L, et al. Granulation of Fe–Al–Ce hydroxide nano-adsorbent by immobilization in porous polyvinyl alcohol for fluoride removal in drinking water, Powder Technol. 209 (2011) 92-97.

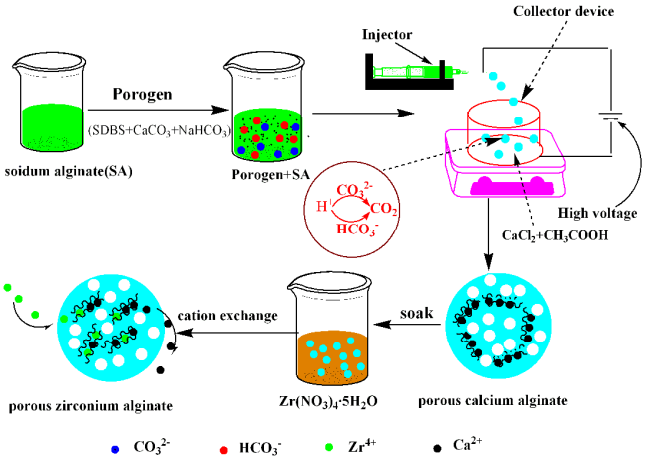

Fig. 1 Schematic diagram of preparation porous zirconium alginate.

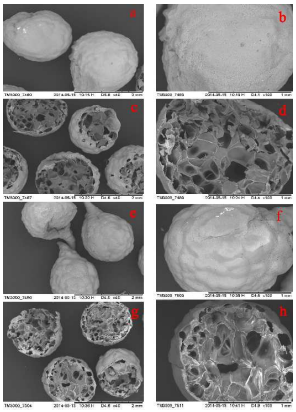

Fig. 2 SEM of porous zirconium alginate beads and its cross section before adsorption (a)-(d) and after adsorption (e)-(h).

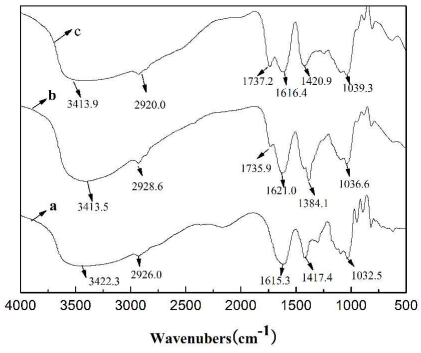

Fig. 3. FT-IR spectra of the samples: (a) sodium alginate, (b) porous zirconium alginate beads before fluoride ion adsorption, (c) porous zirconium alginate beads after fluoride ion adsorption.

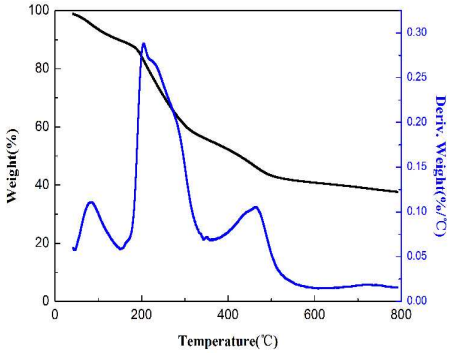

Fig. 4. Thermal analysis curve: TGA and DTA of adsorbent.

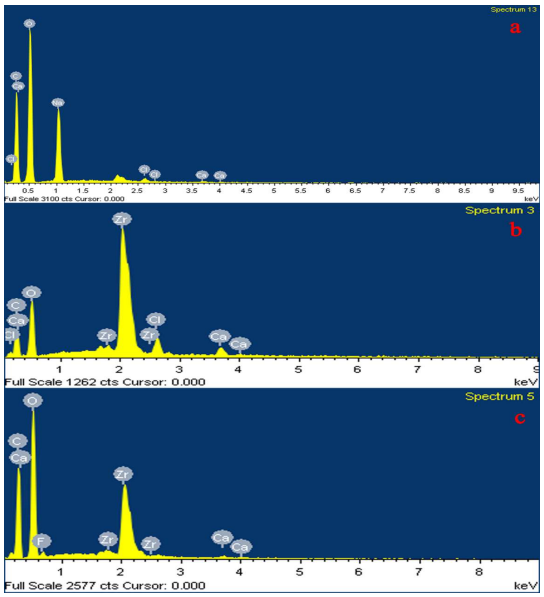

Fig. 5. EDX spectra of sodium alginate beads (a), porous zirconium alginate (b) and fluoride adsorbed porous zirconium alginate beads(c).

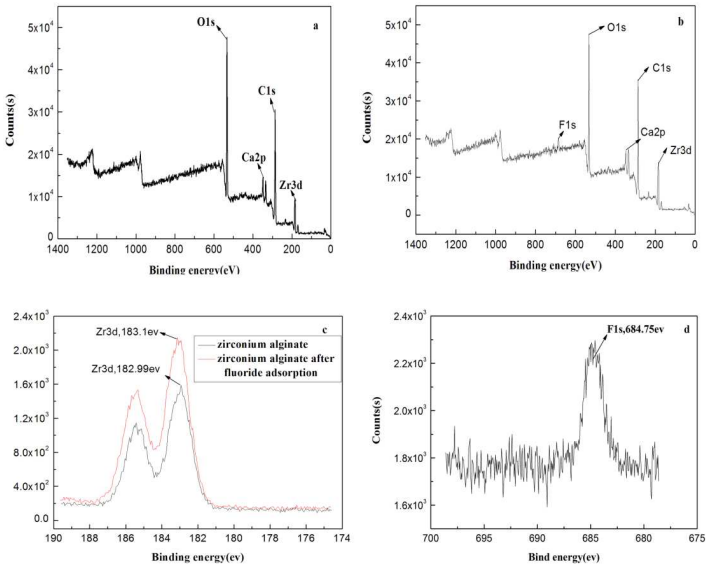

Fig. 6 XPS spectra of (a) porous zirconium alginate beads and (b) porous zirconium alginate beads after fluoride adsorption; XPS spectra of Zr3d before and after fluoride adsorption; XPS spectra of F1s (d).

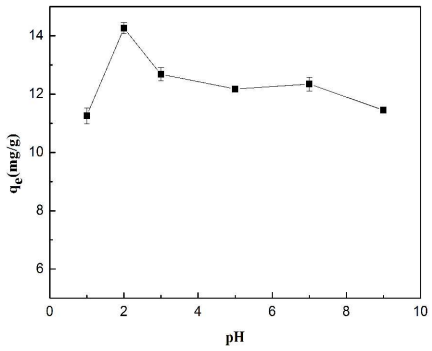

Fig. 7. Influence of pH on the adsorption of fluoride onto porous zirconium aginate beads (Adsorbent dose: 0.05 g; initial fluoride concentration 20 mg/l; contact time 24 h; temperature: 25 □.)

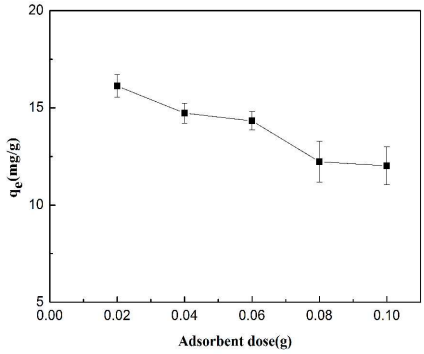

Fig. 8. Effect of adsorbent dose on the adsorption of fluoride onto porous zirconium alginate beads (pH 2; initial fluoride concentration 30 mg/L; contact time 24 h; temperature: 25 □.)

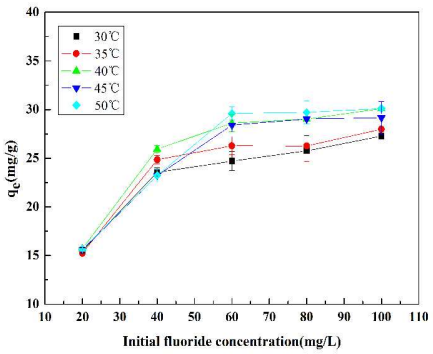

Fig. 9. Effect of initial fluoride concentrationon the adsorption of fluoride onto porous zirconium alginate beads (pH 2; adsorbent dose 0.05g; contact time 24h; temperature: 30□-50□.)

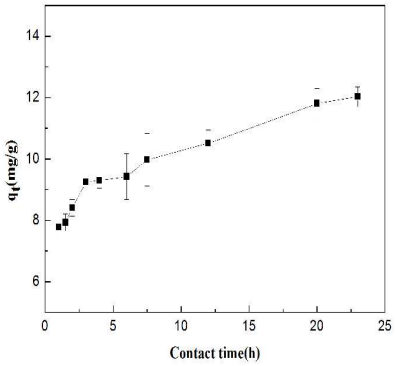

Fig. 10. Effect of contact time on the adsorption of fluoride onto porous zirconium alginate beads (pH 2; adsorbent dose 0.05 g, initial fluoride concentration 20 mg/L; temperature: 25 □.)

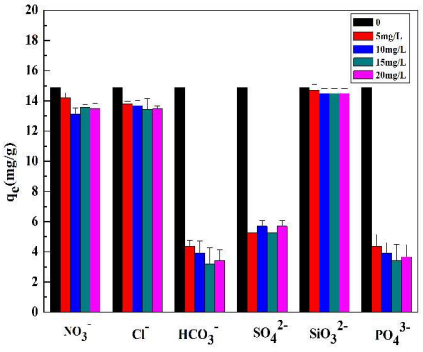

Fig. 11 Effect of co-existing anions on the fluoride adsorption

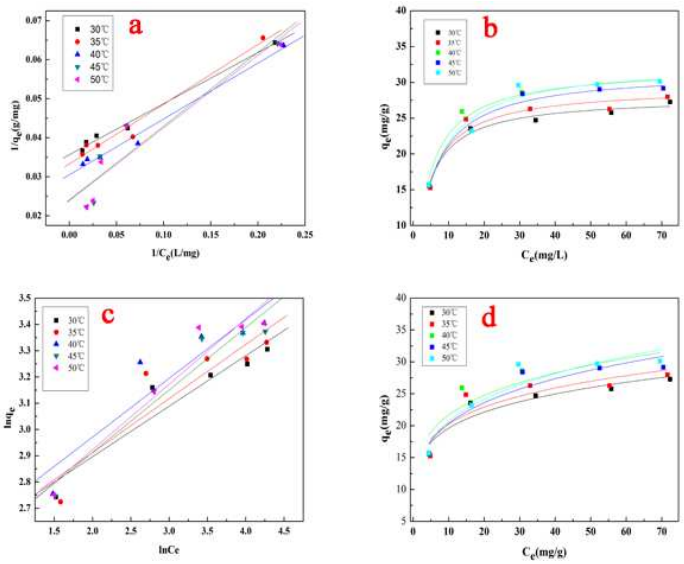

Fig. 12. Langmuir and Freundlich adsorption isotherms model
(a), (b)-the linear and non-linear model of Langmuir; (c), (d)-the linear and non-linear model of Freundlich

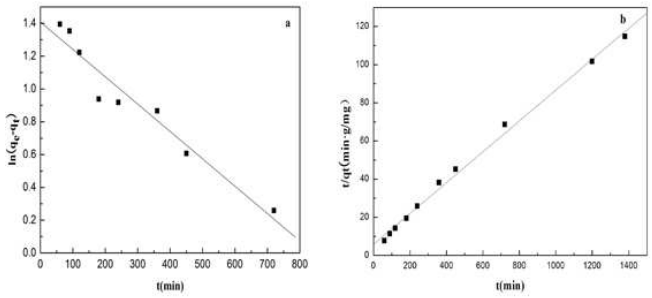

Fig. 13. pseudo-first-order and pseudo-second-order rate model
(a), (b)-the linear of pseudo-first-order model and pseudo-second-order rate model.

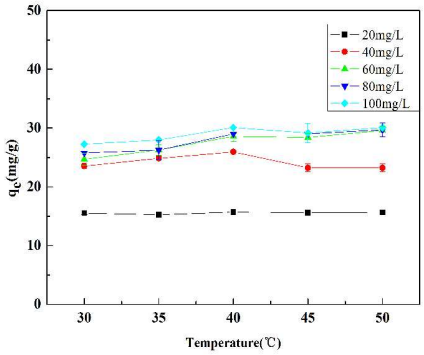

Fig. 14. Effect of temperature on the adsorption of fluoride onto porous zirconium alginate beads (pH 2; adsorbent dose 0.05 g; initial fluoride concentration 20 mg/L; contact time 20 h.)

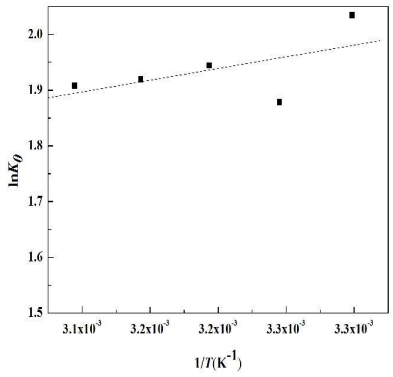

Fig. 15. The plot of lnK_0 versus 1/T for fluoride adsorption on porous zirconium alginate beads

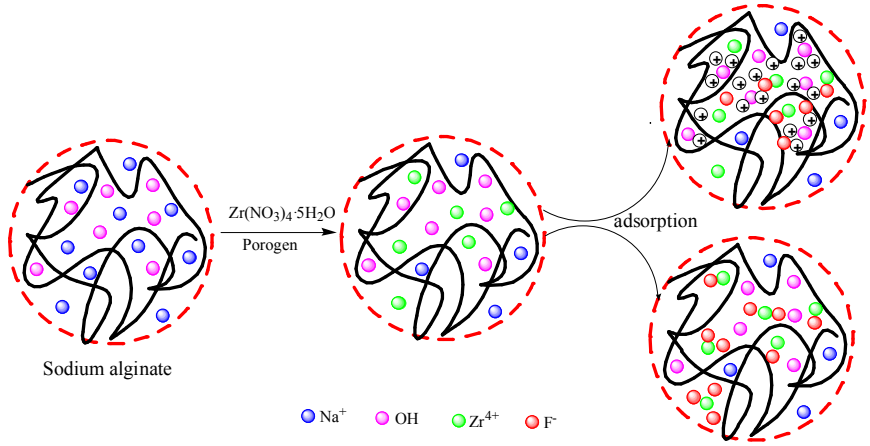

Fig. 16 Mechanism schematic of fluoride adsorption on porous zirconium alginate

Table 1 The parameters of Langmuir and Freundlich model

Type	T(K)	Langmuir			Freundlich		
		q_m/mg·g^{-1}	b/L·mg^{-1}	R^2	K_F/(mg·g^{-1})(L·mg^{-1})$^{1/n}$	n	R^2
Linear model	303.15	28.050	0.273	0.992	12.327	5.201	0.907
	308.15	30.039	0.218	0.974	12.176	4.854	0.824
	313.15	32.797	0.213	0.988	12.471	4.468	0.857
	318.15	31.210	0.218	0.989	11.440	4.206	0.934
	323.15	32.185	0.209	0.979	11.300	4.013	0.928
Nonlinear model	303.15	27.950	0.280	0.976	13.098	5.718	0.869
	308.15	29.360	0.252	0.935	13.453	5.631	0.743
	313.15	32.103	0.241	0.971	13.911	5.207	0.792
	318.15	31.563	0.206	0.972	12.423	4.674	0.882
	323.15	32.737	0.193	0.947	12.352	4.473	0.862

Table 2 parameters for D-R model for the removal of fluoride

q_m (mg/g)	K (mol^2/kJ^2)	E (kJ/mol)	k
13.869	1.196	0.647	1.196

Table 3 The parameters of pseudo-first-order and pseudo-second-order rate model

Model	pseudo-first-order model			pseudo-second-order model		
Parameter	q_e (mg/g)	k_1(g/(mg·min))	R^2	q_e(mg/g)	k_2(g/(mg·min))	R^2
value	4.087	1.67*10^{-3}	0.940	12.379	1.28*10^{-3}	0.995

Table 4 Thermodynamics parameters for the sorption of fluoride ion by zirconium alginate beads

T(K)	ΔH^0(kJ/mol)	ΔS^0(J/(mol·K))	ΔG^0(kJ/mol)
303.15	-3.494	4.855	-5.127
308.15			-4.811
313.15			-5.062
318.15			-5.076
323.15			-5.127

Table. 5. Comparison of various adsorbents for fluoride removal

Adsorbents	c(F^-) (mg/L)	pH	Contact time(h)	Temperature(□)	q_{max} (mg/g)	Reference
Protonated chitosan beads	10	7	0.5	30	1.664	[5]
Mesoporous alumina	5	3	24	30 (±2)	8.264	[27]
Hydrous iron(III)-tin(IV) bimetal mixed oxide	50	6.4±0.2	4	30 (±1.6)	10.5	[36]
Orange waste gel	--	3-5	24	30	23.18	[21]
Hydrous ferric oxide doped alginate beads	35	7	24	29	8.9	[20]
Zr(IV)-immobilized resin	80	3	24	30	6.14	[37]
magnesia-loaded fly ash cenospheres	100	3.0	24	45	6	[7]
alginate entrapped Fe (III)–Zr (IV) binary mixed oxide	10	6.0	3.5	25	0.981	[22]
Fe-Al-Ce trimetal hydroxide	19	6.5	--	--	4.46	[38]
Porous zirconium alginate beads	100	2	20	40	32.797	Present study

"--" represented the information was not given in the references.